

Design of a convection-cooled, cluster-based voltage divider chain for photomultiplier tubes

Xi Bin Gu, Ying Guo, Ed Kawamura, and Ralf I. Kaiser^{a)}

Department of Chemistry, University of Hawaii at Manoa, Honolulu, Hawaii 96822

(Received 6 May 2005; accepted 1 July 2005; published online 4 August 2005)

A highly stable convection-cooled, cluster-based voltage divider chain for photomultiplier tubes has been designed and tested in single ion counting detection systems. Contrasting currently existing voltage divider chains, our unit does not require a cooling liquid to transfer the heat from the resistors and provides safer operation conditions inside ultrahigh vacuum systems utilized in the reaction dynamics community. The unit is enclosed in an air pocket inside an ultrahigh vacuum system so that outgassing of the photomultiplier tubes, resistors, and capacitors can be eliminated completely. The measured resistor chain currents of $\pm 2\%$ lie well within the tolerances of the resistors ($\pm 5\%$) and power supply ($\pm 1\%$) demonstrating that the convective cooling is actually efficient to sustain a stable signal. The monitored total ion current also depicts extremely low fluctuation of only 1.5%. The day-to-day reproducibility has been tested, too. We also demonstrate that a magnetic shielding of the photomultiplier tube and the resistor chain enhances the signal by about 15%. © 2005 American Institute of Physics. [DOI: 10.1063/1.2006671]

I. INTRODUCTION

Photomultiplier tubes present versatile detector elements of low level photon counting in the ultraviolet, visible, and infrared regions of the electromagnetic spectrum.^{1–5} A typical photomultiplier contains a photosensitive surface (photocathode) which is positioned inside a vacuum housing (Fig. 1). A photon passing the transparent photomultiplier faceplate impinges on the photocathode and produces a photoelectron (photoelectric effect). The photoelectron is directed by an electric field to an electrode (dynode, d_1) located inside the photomultiplier housing and generates a cascade of δ secondary electrons. Each of the δ electrons is in turn directed to a second dynode (d_2) which lies at a positive potential with respect to dynode d_1 to cause also n secondary electrons. Several secondary emission stages (dynodes) are coupled together so that the secondary electrons from a dynode (d_n) turn into the primary electrons of the next dynode (d_{n+1}). The net effect is that each primary electron generates an amplified electron cascade. The electrons from the last dynode are collected by an anode which provides the signal current that is fed out. The total gain, μ , of the photomultiplier is given by $\mu = \delta^n$, where δ is the number of secondary electrons emitted per stage and n the number of dynodes.⁶ This treatment assumes a constant number of electrons emitted from each stage; further, all electrons released from dynode n are assumed to be collected by following dynode. Hence, the crucial advantage of a photomultiplier tube is the capability of high gain and large signal amplitude. For instance, in a 12 stage photomultiplier with a secondary emission ratio of 5, the current amplification is about 2×10^8 . Due to this high level of electron multiplication by the dyn-

ode chain, photomultiplier detectors offer high sensitivity to single photons and hence are commonly utilized when the input signal (photons) is pulsed.⁷ Therefore, photomultiplier tubes have wide applications in the chemical dynamics community (photodissociation dynamics, reactive scattering experiments) and are commonly incorporated into mass spectrometric detector systems coupled to Daly-type particle detectors.⁸

However, a proper operation of the photomultiplier depends critically on the stability of the applied voltage to the dynode chain and a constant operation temperature. Here, a small variation in the operation voltage of only 1% can result in a much larger percentage change of up to 10% in the tube gain; this issue can be overcome easily by utilizing highly stable power supplies. The constant operation temperature presents a tricky problem. First, as the temperature increases, the dark current and noise level of the photomultiplier tube are also enhanced (thermo ionic emission from the photocathode). Second, the resistance of the dynode chain resistors depends on the temperature. As the latter rises, the resistance is increased, too; this instability leads to a drift in the amplification rate. To overcome this problem, the photomultiplier tube and resistor chain have to be cooled during the operation to maintain a constant temperature. This has been achieved in previous designs by chilling the photomultiplier tube and resistor chain with circulating dry ice—acetone mixtures, pressurized cold nitrogen gas, and cooling water.⁹ However, if the dynode chain and the photomultiplier tube are housed inside (ultra) high vacuum systems such as crossed molecular beams machines, gas/liquid feedthroughs as well as potential cooling line leaks and ruptures present imminent hazards.

Here, we present a design of a highly stable, convection-cooled cluster-based resistive voltage divider chain for photomultiplier tubes. This design can be easily integrated into

^{a)} Author to whom correspondence should be addressed; electronic mail: kaiser@gold.chem.hawaii.edu

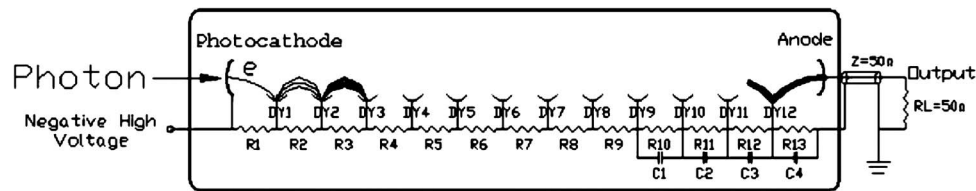


FIG. 1. Circuit diagram of the voltage divider chain. DY refers to the dynodes, R to the resistors, and C to the capacitors.

currently existing ultrahigh vacuum systems such as crossed beams machines,¹⁰ surface scattering vessels,¹¹ and photodissociation setups.¹² Our article is organized as follows. Section II elucidates on the design of the cluster-based voltage divider chain, whereas the incorporation of the voltage divider inside the vacuum system of a crossed molecular beams machine is discussed in Sec. III. The performances of the new module are addressed in Sec. IV.

II. DESIGN OF THE VOLTAGE DIVIDER CHAIN

The pattern of the resistor chain was designed to be interfaced to a Burle 8850 photomultiplier tube and a 21 pin TP-147 socket. The Burle 8850 unit presents a 12 stage, sealed end window, 51-mm-diam photomultiplier employing a semitransparent photocathode and a high-gain gallium-phosphide (GaP) first dynode followed by high-stability copper-beryllium dynodes in the succeeding stages. The 8850 is highly useful for the detection of extremely low-light level measurements in the blue region of the spectrum. Since we incorporate the unit inside an ion counting detector system (single photon counting) of a crossed beams machine (Sec. III), we utilized a circuit diagram for a rapid pulse response time (Fig. 1). The main voltage divider consists of 12 resistors R1–R12 connected to the photocathode and to dynodes DY1–DY12. The resistors were chosen to be 600 k Ω (R1; 5 \times 120 k Ω in series R1A–E), 100 k Ω (R2), 140 k Ω (R3; 100 and 40 k Ω in series; R3A–B), and 100 k Ω (R4–R13). We would like to elucidate briefly on the choice of the resistor type. In pulse counting mode, up to -3 kV can be applied between the cathode and the anode. Considering the total resistance of the circuit of 1.83 M Ω with a current of 1.64 mA, 4.9 W of heat will be generated in the resistor chain. Metal oxide power resistors (Xicon MO Series) present an ideal choice. First, the temperature coefficient of the 5 W series of only ± 350 ppm K $^{-1}$ guarantees stable operation conditions. Second, the soldering of these resistors adds only 0.05 Ω per solder joint to the total resistance. Finally, a fast rise and response time allows even counting rates up to the MHz regime. On the other hand the physical size of the resistors of a length of 25 mm and diameter of 8 mm presents challenging design criteria of the resistor chain (Figs. 2 and 3).

In addition to the resistors, we added four ceramic capacitors C1–C4 (rated for 1 kV) to the resistor chain (C1 = 0.005 μ F, C2 = 0.015 μ F, C3 = 0.02 μ F, C4 = 0.05 μ F). Why are these capacitors crucial? In applications in which the input signal is pulsed such as in ion counting systems, the averaged anode current is determined by the peak pulse current and the peak width. If the average anode current is much less than the peak pulse current, the dynode potentials can be

maintained at an almost constant value during the pulse operation mode by using charge storage capacitors at the tube socket (Figs. 2 and 3). The voltage divider current needs to be only sufficient to provide the average anode current for the photomultiplier tube. High peak currents required during the large amplitude pulses are supplied by the capacitors.¹³ The present design limits the voltage change across the capacitor to 1% during the pulse. The capacitors are not crucial across those dynodes at which the peak current is less than 10% of the average current (DY1–DY9).

How are the resistors and capacitors actually assembled to a unit? The schematic side view of the voltage divider chain is shown in Fig. 2; Fig. 3 depicts the two- and three-dimensional assembly drawings of the unit. The resistors are arranged in an inner (R1A–E) and in an outer (R2–R13) ring around the axis of the cylinder-shaped module (length = 6 cm; diameter = 6 cm). Two boards sandwich the resistor clusters and interface the latter with the capacitors to the photomultiplier socket (Fig. 4). Due to geometrical limitations, two capacitors C1 and C2A are connected above the resistor clusters, whereas capacitors C2B, C3, and C4 are connected to the lower board. Three threaded rods secure the photomultiplier socket and boards. Since the design of the resistive chain is very compact and versatile, it can be adapted to any photomultiplier—not only to the Burle 8850 type—simply by exchanging the photomultiplier socket and adjusting the resistors and capacitors.

III. INCORPORATION OF THE MODULE INTO THE VACUUM SYSTEM

The module is incorporated into a recently commissioned universal crossed beams machine. Briefly, the main chamber of the crossed beams machine consists of a 304 stainless steel box (180 cm \times 160 cm \times 80 cm; 2300 l) and is evacuated by three 2000 l s $^{-1}$ magnetically suspended turbo-

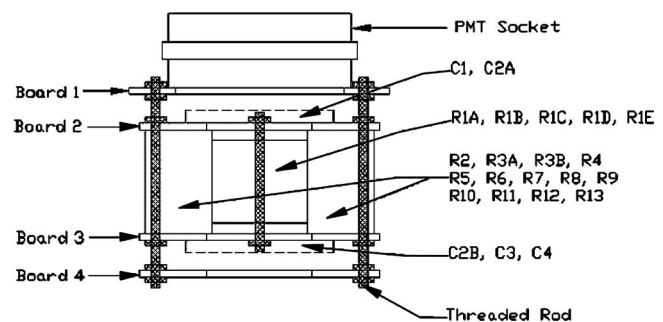


FIG. 2. Schematic side view of the voltage divider chain. DY refers to the dynodes, R to the resistors, and C to the capacitors. Due to geometrical limitations, C2 is split up (C2A, CB)

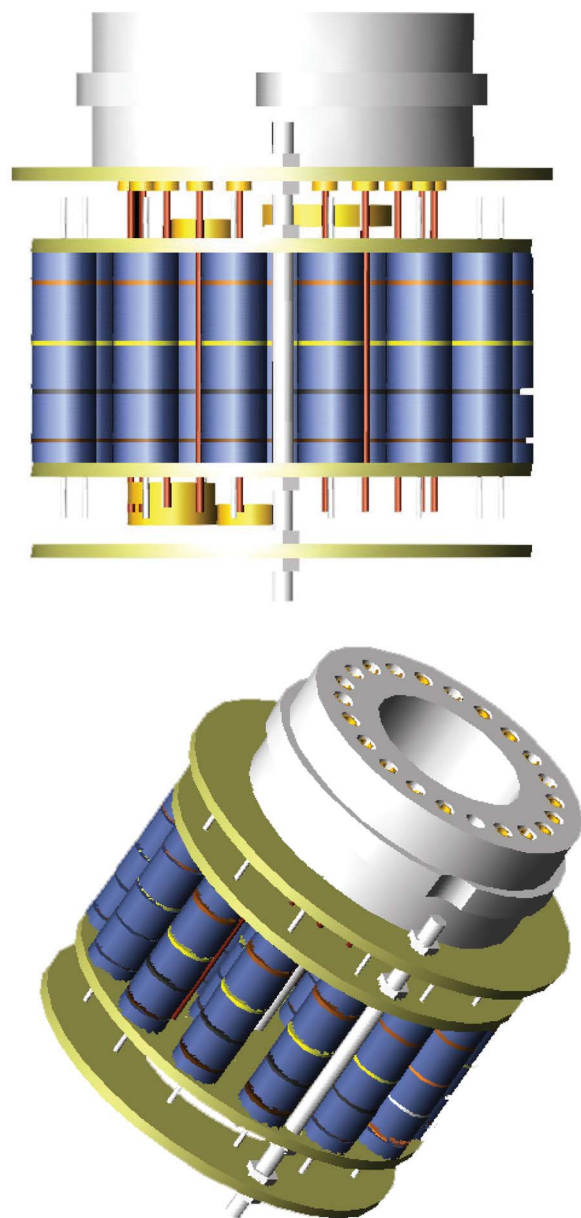


FIG. 3. (Color) Assembly drawing of the voltage divider chain (left: side view; right: three-dimensional view). DY refers to the dynodes, R to the resistors, and C to the capacitors.

molecular pump (Osaka Vacuum; TG 2003) backed by a single scroll pump (Edwards XD35; 10 l s^{-1}) to the low 10^{-8} Torr region. To reduce the background from straight-through molecules into the detector, the machine is also equipped with a cold shield located between the chopper wheel and the interaction region and downstream of the skimmer (secondary source). This oxygen free high conductivity copper shield is interfaced to the first stage (10 K) of a CTI CP-1020 cold head (4500 l s^{-1} (water); 1500 l s^{-1} (nitrogen/oxygen) and improves the vacuum in the main chamber to 4×10^{-9} Torr. This arrangement keeps the pressure in the main chamber during an actual experiment to 10^{-7} Torr (continuous sources) and 5×10^{-8} Torr (pulsed sources). Two source chambers are located inside the main chamber; in its current geometry, both beams cross perpendicularly. Each source chamber is pumped by a 2000 and a

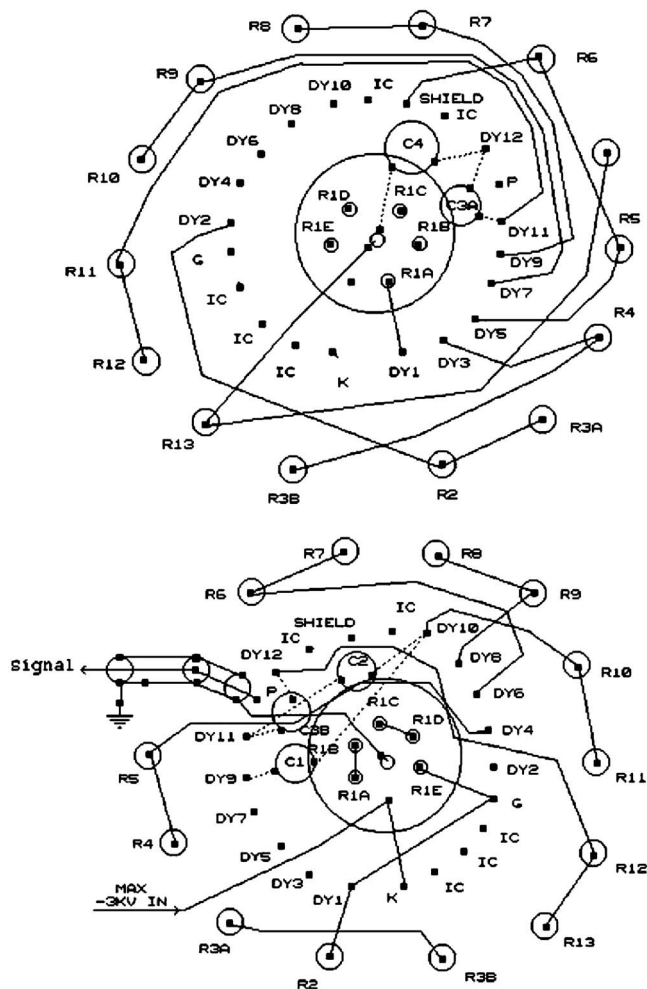


FIG. 4. Circuit layout of board 1 (top) and board 2 (bottom). Please refer to the text for details on the resistors and capacitors.

430 l s^{-1} maglev pump (Osaka Vacuum; TG2003 and TG430) to the low 10^{-8} Torr region; operating pulsed and continuous sources increases the pressure to about 10^{-5} and 10^{-4} Torr, respectively. All maglev pumps require no maintenance and are hydrocarbon free. A dry roots pump (Leybold WS505; 140 l s^{-1}) roughed by two oil-free EcoDry M30 pumps (Leybold; 16 l s^{-1}) backs the turbo pumps of each source chamber. To minimize the outgassing of the sealing material, copper gaskets are used preferentially. Whenever O rings are used (detector entrance port, main door), these are Teflon coated and differentially pumped by an oil-free pumping station at 5×10^{-8} Torr to ensure the 4×10^{-9} Torr in the main chamber.

The species—either reactively scattered or those from an on-axis velocity calibration of a parent beam—are monitored using a quadrupole mass spectrometer (Extrel). Actually, the detector is located in a separate, triply differentially pumped ultrahigh vacuum chamber (10^{-11} Torr) and is rotatable within the plane defined by both beams. Since every rotation in a vacuum system will increase the pressure, the rotating detector ring is separated by three Teflon loaded seals from the atmosphere. The spaces between these seals are doubly differentially pumped to reduce the pressure from atmosphere (760 Torr) via 10^{-2} and 4×10^{-8} Torr (Teflon sealed

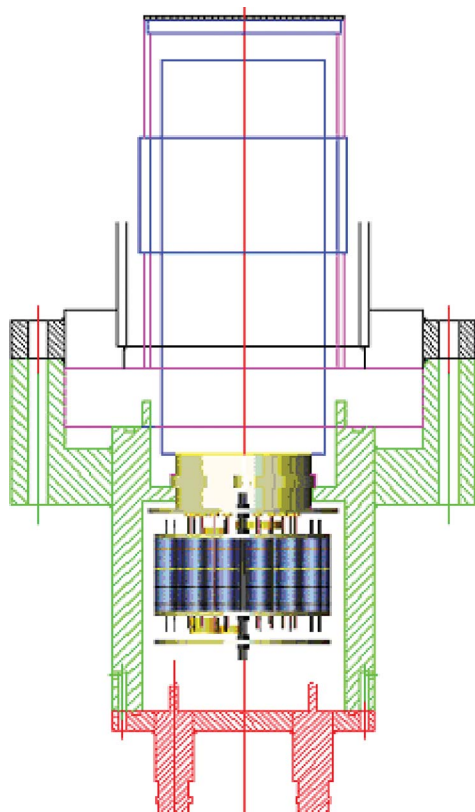


FIG. 5. (Color) Side view of the conflate flange based photomultiplier housing together with the photomultiplier tube, and resistor chain.

regions) to 4×10^{-9} Torr in the main chamber. This arrangement ensures no pressure increase in the main chamber even if the detector is being rotated. Differentially pumped detector regions I/II reduce the gas load from the main chamber, whereas region III contains the Brink-type electron impact ionizer,¹⁴ surrounded by a liquid nitrogen cold shield. The quadrupole mass filter and the Daly-type scintillation particle detector¹⁵ are connected to region II. Each region is pumped by a magnetically levitated turbo-molecular pump (region I/II: TD411, 430 l s^{-1} ; region III: TD 400: 300 l s^{-1}); all three pumps are backed by a 430 l s^{-1} turbo-molecular pump whose exhaust is connected to an oil-free scroll pump (Edwards XD35; 10 l s^{-1}). This pumping scheme reaches down to the low 10^{-11} Torr in region III; lower pressures can be achieved by operating a cold head inside region III (Sumitomo; RDK-415 E; 4 K; 1.5 W). A slide valve with a Teflon coated O ring is used to separate the main chamber from the first differentially pumped detector region.

We concentrate now on the incorporation of the newly designed voltage divider chain into the detection system (Fig. 5). Recall that the actual ionizer consists of a thoriated iridium filament spot welded to a gold plated stainless steel cylindrical can, a meshed wire grid, and an extractor lens held at -150 V . Note that we incorporated a four lead circuit, i.e., feeding two instead of one wire to the anode and cathode of the filament, respectively. This circuit eliminates the resistance of the leads to the filament and hence minimizes voltage drops. The reduced voltage drop in turn minimized the heat released from the filament to typically 6.3 W (1.8 V and 3.5 A for 1 mA emission current). The electron energy, i.e.,

the potential difference between the can and the grid, was held at 200 eV , whereas the ion energy was held at $+36 \text{ eV}$. The extracted ions pass the entrance lens of the quadrupole rods (-140 V), are separated in the quadrupole system, leave the exit lens (-140 V), and are accelerated towards an aluminum coated stainless steel target maintained at -25 kV . The ion hits the surface and initiates an electron cascade which is accelerated toward an aluminum coated (200 nm) organic scintillator BC-418 (Saint Gobain; 391 nm photon emission). This process generates a photon pulse inside the scintillator; the photons pass through the quartz window of the photomultiplier housing, enter the photomultiplier tube located outside the ultrahigh vacuum system (Fig. 5), and interact with the photocathode to initiate a photoelectron, cf. Sec. I. To avoid dark currents via field emission, both the electrically insulated aluminum coating of the scintillator and the first dynode are at the same potential. The actual photomultiplier housing (Larson Electronic Glass) consists of conflate flange (polished to the high vacuum side) which is interfaced via an insulating glass tube to a stainless steel tube; the latter is sealed by a quartz plate holding the aluminum coated, organic scintillator. Therefore, the photomultiplier housing actually separates the ultrahigh vacuum of detector region II from the high vacuum of the main chamber. The photomultiplier tube is interfaced via the Teflon socket to the newly designed resistor chain (Sec. II). Each photomultiplier pulse passes a discriminator (discriminator level: $1.0\text{--}4 \text{ mV}$). Here, an amplification by the dynode chain of about 3×10^7 combined with a pulse width of about 10^{-8} s produces a current of about 0.5 mA . A 50Ω termination gives rise to pulse amplitudes of 20 mV . The pulse is amplified and converted into a TTL pulse; the latter is fed into a multichannel scaler (dwell time of each channel between 0.64 and $10.24 \mu\text{s}$).

Having addressed the position of the photomultiplier tube and the cluster-based resistor chain, we finally address how to dissipate the heat (4.9 W at 3 kV) generated in the resistor chain. Recall that a stable, low temperature is crucial to ensure a low dark current. Also, any temperature increase would also translate into an increased resistance of the ceramic insulators which in turn changes the total gain of the photomultiplier tube. To eliminate any temperature increase, both the photomultiplier tube and the resistor chain are sealed via an O-ring tightened flange inside the photomultiplier housing. This design actually provides a sealed air pocket in which the photomultiplier tube and the resistor chain are enclosed. This air pocket guarantees a cooling of the resistors via convection to the stainless steel housing hence eliminating an increase of the temperature and resistance during the operation of the photomultiplier. The convection based design removes the necessity to cool the resistor chain with liquids or cooled gases hence ensuring safer and more stable operation conditions of photomultiplier tubes in the field of reaction dynamics.

IV. PERFORMANCE

We will demonstrate now the performance of the resistor chain. First, we tested the resistor current through the resistor

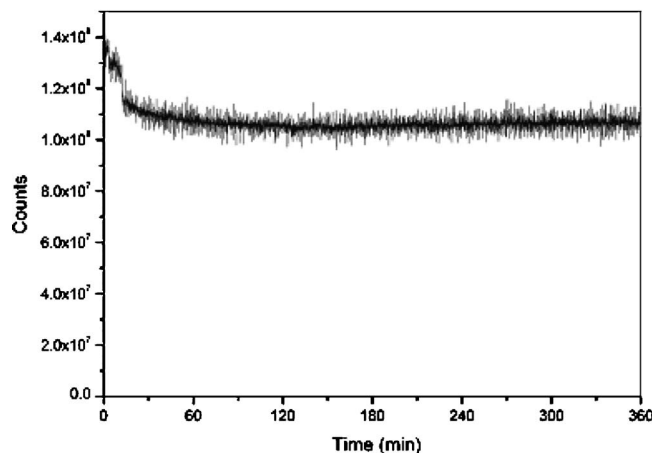


FIG. 6. Total ion current in our mass spectrometer from $m/e=2$ to $m/e=100$ versus the time.

chain at voltages of 1.5, 2.5, and 2.9 kV. We monitored 0.820, 1.09, and 1.36 mA. This compares nicely with the theoretical value of 0.85, 1.12, and 1.40 mA; the deviation of typically 0.02 mA ($\pm 2\%$) is well within the nominal resistor ($\pm 5\%$) and power supply ($\pm 1\%$) accuracies. This demonstrates that the convective cooling system is working as anticipated since an inefficient heat transfer would have resulted in a temperature increase of the resistors; this in turn would have translated into a higher resistance and hence lower current which was clearly not observed. As a side result, the enclosure of the photomultiplier tube and resistor chain prevent an outgassing into the high vacuum system of the main chamber. Second, we showed the long-term stability of the resistor chain by monitoring the total ion current in our mass spectrometer from $m/e=2$ to $m/e=100$ versus the time (Fig. 6). Note that the system requires 90 min to stabilize [power supplies of the photomultiplier tube and of the high voltage target (Daly detector); temperature transfer from the resistor chain]. Here, the fluctuations are within 1.5% suggesting a very stable operation of the system.

The stability of the convection-cooled resistor chain allowed us also to investigate the effect of the Earth's magnetic field on the performance of the photomultiplier tube. Note that Earth's magnetic field affects the trajectories of the photoelectrons from the photocathode to the first dynode.¹⁶ We recorded 5120 time-of-flight (TOF) spectra of a neat helium beam (900 Torr backing pressure; continuous source with a 0.1 mm nozzle; nozzle—skimmer distance: 6 mm; 50 s data accumulation time; ground state helium atoms) operating the photomultiplier tube at -1.15 kV, the discriminator at 1.0 mV, and the ionizer at an emission current of 1 mA; the four-slotted chopper wheel located between the skimmer and the entrance aperture (0.25 mm) to region I of the detector was held at 100 Hz. Figure 7 depicts the TOF spectra with (0.1 mm μ metal) and without magnetic shielding. It is clearly evident that the magnetic shielding increases the signal by about 15%. This underlines the necessity to magnetically shield the photomultiplier tube carefully.

V. SUMMARY

We presented the design and performance of a highly stable convection-cooled, cluster-based voltage divider chain

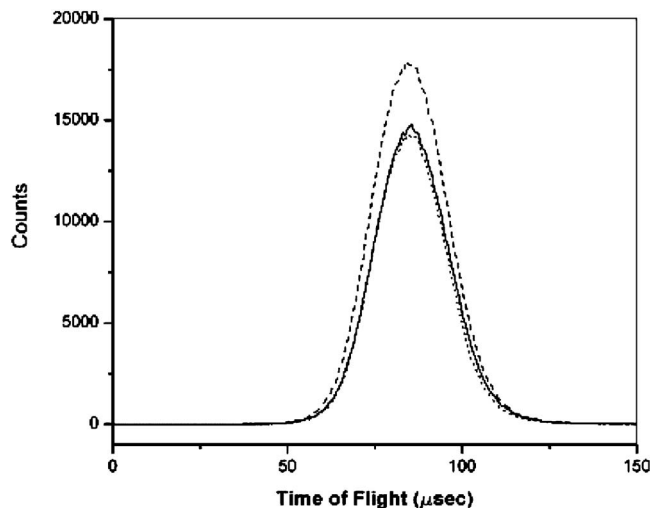


FIG. 7. Time-of-flight spectrum of a continuous helium beam recorded with magnetic shielding of the photomultiplier tube and resistor chain (dashed line), shielding of only the resistor chain (solid line), and without shielding (dotted line).

for photomultiplier tubes. Compared to currently existing voltage divider chains, this unit does not require a cooling liquid to transfer the heat from the resistors and provides safer operation conditions inside ultrahigh vacuum systems utilized in the reaction dynamics community. The cylindrical unit is enclosed in an air pocket inside an ultrahigh vacuum system so that outgassing of the photomultiplier tubes, resistors, and capacitors can be eliminated completely. The measured resistor chain currents of $\pm 2\%$ lie well within the tolerances of the resistors ($\pm 5\%$) and power supply ($\pm 1\%$) demonstrating that the convective cooling is actually efficient to sustain a stable signal. The monitored total ion current also depicts extremely low fluctuation of only 1.5% after the system has been equilibrated for 90 min demonstrating that the resistor chain is highly stable over extended times. Finally, we showed that shielding the photomultiplier tube and the resistor chain can enhance the signal by about 15%.

ACKNOWLEDGMENTS

This work was supported by the U.S. Department of Energy-Basic Energy Sciences (DE-FG02-03ER15411; X.G., R.I.K.) and by the National Science Foundation (CHE-0234461; Y.G., R.I.K.).

¹M. D. Seltzer, M. Schulz, H. Hendrick, and R. G. Michel, *Anal. Chem.* **57**, 1096 (1985).

²F. Muheim, *Nucl. Instrum. Methods Phys. Res. A* **502**, 52 (2003).

³I. S. McDermid, T. D. Walsh, A. Deslis, and M. L. White, *Appl. Opt.* **34**, 6201 (1995).

⁴D. B. Harper and R. J. DeYoung, NASA Special Publication NASA/TM-1998-207674.

⁵M. C. Piton and W. Panning, *Rev. Sci. Instrum.* **61**, 3726 (1990).

⁶D. R. Carter, *Photomultiplier Handbook—Theory, Design, and Application* (Burle Technologies, Lancaster, 1988).

⁷G. Scoles, *Atomic and Molecular Beam Methods* (Oxford University Press, Oxford, 1992), Vols. 1 and 2.

⁸X. Yang and K. Liu, *Modern Trends in Chemical Reaction Dynamics* (World Scientific, Singapore, 2004).

⁹J. H. Moore, C. C. Davis, and M. A. Coplan, *Building Scientific Apparatus* (Perseus, Cambridge, 2003).

¹⁰R. I. Kaiser, *Chem. Rev. (Washington, D.C.)* **102**, 1309 (2002).

- ¹¹R. A. Dressler, *Chemical Dynamics in Extreme Environments* (World Scientific, Singapore, 2001).
- ¹²K. Liu and A. Wagner, *The Chemical Dynamics and Kinetics of Small Radicals* (World Scientific, Singapore, 1995).
- ¹³P. S. Aplin, *Meas. Sci. Technol.* **8**, 340 (1997).
- ¹⁴G. O. Brink, *Rev. Sci. Instrum.* **37**, 857 (1966).
- ¹⁵N. R. Daly, *Rev. Sci. Instrum.* **31**, 264 (1960).
- ¹⁶A. Tripathi, K. Arisaka, T. Ohnuki, and P. Ranin, University of California, Los Angeles, Report No. 2001-04.